Physics of the Solid State, 2024, Vol. 66, No. 8

02

Andreev bound states and paramagnetic effect at low temperatures in YBCO thin films

© E.A. Arkhipova[1], A.I. El'kina[1], D.V. Masterov[1], S.A. Pavlov[1], A.E. Parafin[1], E.E. Pestov[1], P.A. Yunin[1,2], D.A. Savinov[1,2,¶]

[1] Institute of Physics of Microstructures, Russian Academy of Sciences, Nizhny Novgorod, Russia
[2] Lobachevsky State University, Nizhny Novgorod, Russia
[¶] E-mail: savinovda@ipmras.ru

Received April 18, 2024
Revised April 18, 2024
Accepted May 8, 2024

In this work, non-contact studies of a series of thin epitaxial $YBa_2Cu_3O_{7-x}$ (YBCO) films with different orientations of the a and b axes relative to the film boundaries were carried out. The thicknesses of the films ranged from 2 to 20 nm. From the induction measurements, an anomaly low-temperature increase in the London penetration depth λ was observed for several samples below 7−8 K up to 1 K. Within the method of nonlinear near-field microwave microscopy, an increase in the nonlinear microwave response was observed with a decrease in temperature for the samples with the smallest thickness. The experimental results obtained can be related to the presence of Andreev bound states localized near the film boundaries with a certain orientation relative to a and b axes. The presence of these states leads to a paramagnetic effect at low temperatures. The effects of film boundaries and the film thicknesses are discussed.

Keywords: YBCO thin films, London penetration depth, nonlinear response, third harmonic power, Andreev bound states, paramagnetic effect at low temperatures.

DOI: 10.61011/PSS.2024.08.59038.53HH

1. Introduction

It is well known that external magnetic field H is screened effectively in the bulk of the sample (Meissner effect) when a superconductor is cooled below critical temperature T_c [1]. However, magnetic field induction B in a thin near-surface layer is nonzero and has a certain spatial distribution. Superconducting currents are distributed in the same layer, establishing diamagnetism of the bulk superconductor. The characteristic thickness of this layer is specified by London penetration depth λ that depends strongly on temperature T. When T goes below T_c, dependence $\lambda(T)$ decreases monotonically for all superconductors. At sufficiently low T values, the behavior of $\lambda(T)$ may depend on the type of pairing in a superconductor. In the case of conventional s-wave pairing, the $\lambda(T)$ dependence has the following character: $\Delta\lambda(T)/\lambda(0) \propto \exp(-\Delta_0/T)$, where $\Delta\lambda(T) = \lambda(T) - \lambda(0)$ is the London penetration depth shift and Δ_0 is the gap on the Fermi surface at $T = 0$ (see, e.g., [1]). In the case of unconventional pairing of the d-wave nature, a step $\lambda(T)$ dependence is formed at low temperatures. Depending on the quality of the sample and the density of defects, it may be linear or quadratic [2]. Thus, meaningful data on the nature of superconducting pairing may be extracted via direct measurements of low-temperature features of $\lambda(T)$.

The mentioned low-temperature differences between s-wave and d-wave superconductors may be difficult to detect in real experiments performed, e.g., using the inductive method of measuring the London penetration depth [3], since the formulae for both s- and d-wave superconductors may fit in certain cases the observed low-temperature behavior of the London penetration depth [4]. Though, the experimental determination of d-wave type pairing via measurements of temperature dependence $\lambda(T)$ becomes more efficient when the so-called Andreev bound states [5] are present in the quasi-particle excitation spectrum of the superconductor. These states emerge due to the fact that special trajectories of motion of quasi-particles arise near certain boundaries (a specially oriented geometrical sample boundary or a twin boundary) in d-wave superconductors. A quasi-particle initially moves in a positive pairing potential (phase φ of superconducting order parameter $\Delta\exp(\varphi)$ is zero). Following reflection from the corresponding boundary, the trajectory changes so that the quasi-particle starts moving in a negative pairing potential; i.e., phase φ becomes equal to π (the reverse process is also possible). These processes induce the emergence of states corresponding to strictly zero energy in the spectrum of quasi-particle excitations (see [5] for details). These states are called Andreev bound states and are localized within several coherence lengths of the corresponding boundary. Thus, the quasi-particle excitation spectrum of a superconductor with d-wave pairing may contain special states of this kind only in the vicinity of certain boundaries; such states are not found in the spectrum far from the boundaries. Andreev states are actually a direct consequence of a sign change of the order parameter in d-wave superconductors. This is the reason why their formation near geometric boundaries is impossible in s-wave superconductors, where the sign of the order parameter always remains unchanged.

Let us discuss the specifics of orientation of boundaries in d-wave superconductors that are optimal for the formation of Andreev bound states. This orientation of boundaries is specified by their mutual positioning relative to superconductor axes a and b lying in plane (ab), where the sign of the superconducting order parameter changes upon a change in the azimuthal angle. The modulus of order parameter Δ (the energy gap in the spectrum of quasi-particle excitations of a superconductor) is maximized along axes a and b. The value of Δ is minimized along the lines oriented at an angle of 45° to axes a and b and drops to zero at $T = 0$. These directions are called nodal ones. Axis c of the superconductor is oriented perpendicular to plane (ab), and the polar angle is normally measured relative to it. The lattice constants of the superconductor may be determined in space (abc) along the corresponding axes a, b, and c. High-temperature superconducting (HTSC) compound $YBa_2Cu_3O_{7-x}$ (YBCO), which is a superconductor with d-wave pairing, has the following values of lattice constants along axes a, b, and c in the orthorhombic phase: 3.828 Å, 3.888 Å and 11.65 Å, respectively [6]. The conditions most favorable for the formation of Andreev bound states in the quasi-particle excitation spectrum of a superconductor are established near the boundary with orientation [110]. One of the nodal directions is perpendicular to this boundary, and axes a and b are oriented at an angle of 45° to it. These states also emerge at any acute angle between the boundary and axis a (or b). However, such states are lacking in the case of more trivial boundary orientations (e.g., [100] or [010]) with axes a and b being aligned strictly with the boundary and/or perpendicular to it. The trajectories of quasi-particles before and after reflection then correspond to the same phase of the order parameter. The considered special cases were examined in detail in [5] based on the solution of non-stationary Bogoliubov–de Gennes equations. The dI/dV conductivity peak at zero bias (voltage $V = 0$), which is observed near certain specially oriented boundaries of YBCO films [7], provides direct experimental confirmation of the presence of Andreev bound states.

These states may affect the screening of the external magnetic field, which is particularly significant at low temperatures. Andreev states produce the following contribution to the density of states: $N(\varepsilon) \propto \delta(\varepsilon)$ (see [5] for details and review [8]). Inserting this dependence into the expression for London penetration depth shift $\Delta\lambda(T) = \lambda(T) - \lambda(0)$ (see, e.g., [9] and references therein)

$$\frac{\Delta\lambda(T)}{\lambda(0)} = -\int_{-\infty}^{\infty} \frac{N(\varepsilon)}{N(0)} \frac{\partial f}{\partial \varepsilon} d\varepsilon, \quad (1)$$

we obtain $\lambda(T) \propto \frac{1}{T}$, where $f = \frac{1}{1+\exp(\varepsilon/k_B T)}$ is the Fermi–Dirac function, $\varepsilon = E - E_F$ is the quasi-particle energy, and E_F is the Fermi energy. This hyperbolic dependence of the London penetration depth, which is typically observed at low temperatures, corresponds to the formation of paramagnetic currents flowing near the boundary. These currents affect the screening properties of the superconductor, which is manifested as an increase in λ with a reduction in T. The observation of these states appears to be extremely important, since such studies allow one to draw more reliable conclusions concerning the type of superconducting pairing in a certain material.

Andreev bound states were detected by measuring the temperature dependence of the London penetration depth in YBCO-based samples in a number of experiments (see, e.g., [9,10]). In the cited works, boundaries with a special orientation relative to axes a and b were formed through the use of single-crystal samples with a complex geometry [9] and irradiation with individual high-energy ions at certain angles [10]. As a result, an increase in the London penetration depth was observed in the experimental $\lambda(T)$ dependence at temperatures below 10 K.

Moreover, Andreev states induce significant changes in the nonlinear response of superconductors at low temperatures. At sufficiently high external field strengths H, London penetration depth λ becomes a function not only of temperature T, but also of field strength H. This is the nonlinear Meissner effect [11,12], which enables the study of both linear and nonlinear properties of superconductors. In d-wave superconductors, the nonlinear response should intensify with decreasing temperature in accordance with the $1/T$ law; in s-wave superconductors at low temperatures, it is not observed [12]. It is problematic to detect these low-temperature features in actual experiments with YBCO-based epitaxial films. This may be attributed to spatial fluctuations of film axes a, b, and c; natural inhomogeneities; and certain technical limitations of the available measurement equipment. Specifically, there is an upper limit on the reference signal amplitude and a lower limit on temperature, which is usually set at the boiling point of liquid helium (4.2 K). In the presence of Andreev bound states in a d-wave superconductor, the nonlinear response enhancement at lower T is much more profound and follows a power law in $1/T$ (see [13] for details). As was demonstrated in [13], the nonlinear response (supercurrent at the third harmonic of the fundamental frequency) appears to be proportional to integral

$$\eta = \int_{-\infty}^{\infty} N(\varepsilon) \frac{\partial^3 f}{\partial \varepsilon^3} d\varepsilon. \quad (2)$$

It was already noted that Andreev bound states produce the following contribution to the density of states: $N(\varepsilon) \propto \delta(\varepsilon)$. Inserting this dependence into expression (2), we find $\eta_3 \propto \frac{1}{T^3}$.

Thus, Andreev bound states can contribute to the experimental observation of a nonlinear low-temperature response

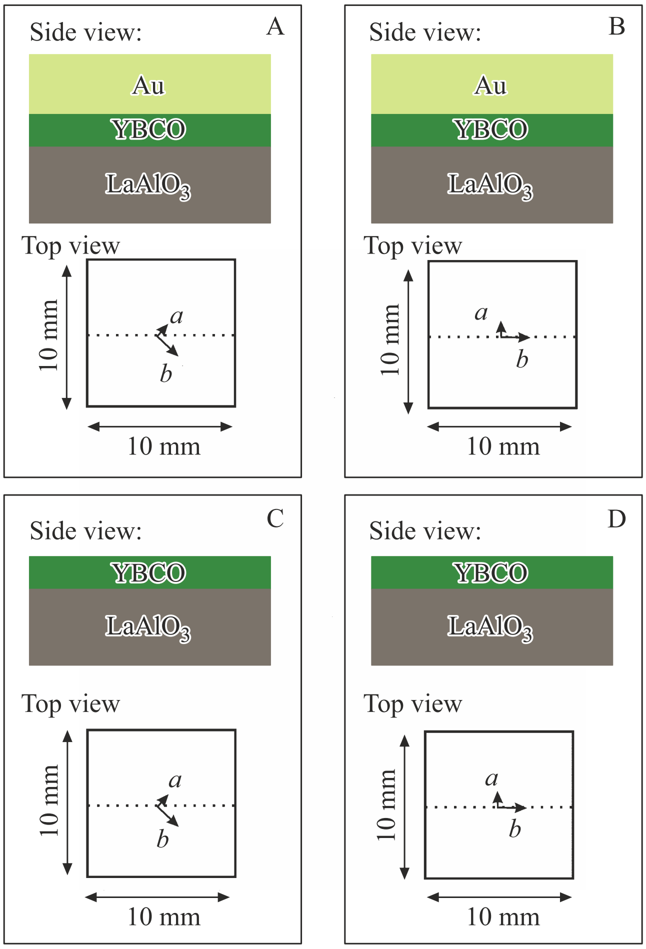

Figure 1. Schematic diagrams of investigated samples type A, B, C, and D.

in epitaxial films of YBCO and other HTSC compounds. This technique for determination of superconducting pairing is an alternative to studying the linear properties of superconductors (measuring temperature dependence of the London penetration depth $\lambda(T)$ [3]). However, low-temperature features of the nonlinear response could not be detected in certain HTSC samples with optimally oriented boundaries (axes a and b oriented at an angle of 45° to the boundaries). In the present study, the nonlinear response of YBCO thin films is investigated locally with the use of a specialized technique: nonlinear near-field microwave microscopy. We observe an increase in the nonlinear microwave response at low temperatures in films with optimally oriented boundaries. The presented experimental results agree with the data obtained using the inductive method of measuring the temperature dependence of the London penetration depth.

2. Preparation of samples

Four types of samples were considered in the present study: type A (square two-layer YBCO/Au structures with axes a and b of the YBCO film oriented at an angle of 45° to the boundaries), type B (square two-layer YBCO/Au structures with axes a and b of the YBCO film directed along/perpendicular to the boundaries), type C (YBCO film with axes a and b oriented at an angle of 45° to the boundaries), and type D (YBCO film with axes a and b directed along/perpendicular to the boundaries). All samples were deposited onto a lanthanum aluminate $LaAlO_3$ substrate. Their schematic diagrams are shown in Figure 1. The thickness of YBCO films varied from $d = 2$ nm to $d = 20$ nm. The thickness of the upper Au layer (for samples type A and B) was 20 nm. Technical limitations of the available nonlinear near-field microwave microscopy setup made it impossible to distinguish the signal from noise at low temperatures in measurements of thicker films. In addition, the nonlinear signal depends strongly on the supercurrent density, which decreases with increasing film thickness; therefore, the nonlinear response is suppressed significantly at low temperatures. The small thickness of YBCO films chosen for examination by the inductive method is attributable to strong magnetic field screening, which also poses the problem of isolating the useful signal from noise. Moreover, paramagnetic currents may be distinguished from diamagnetic ones only with sufficient suppression of the latter. This imposes even more stringent restrictions on the thickness of YBCO films.

Let us discuss the specifics of fabrication of samples type A and B. A YBCO film with certain thickness d was deposited onto the $LaAlO_3$ substrate in the form of a disk 32 mm in diameter. Having performed X-ray diffraction experiments, we examined the orientation of axes a and b in the film. It was then needed to form optimally oriented film boundaries that are as smooth as possible. A layer of gold with a thickness of 20 nm was deposited for this purpose onto the YBCO film. In order to immobilize the sample for further processing, it was glued with wax to a special plate (the upper Au layer was in contact with the plate). Next, cuts needed to form a 10 mm × 10 mm square in the horizontal plane were made with a diamond scriber on the back side of the substrate under a microscope. The structure was then peeled off, wax was removed, and the sample was cleaved mechanically along the cuts. Thus, we obtained a series of square bilayers of types A (thickness $d = 20$, 17, 10, 6, and 2 nm) and B (thickness $d = 2$ nm).

Samples type C and D were prepared in a simpler way. A YBCO film with thickness $d = 4$ nm was deposited onto a pre-cut square $LaAlO_3$ substrate 10 mm × 10 mm in size. Type C and D films differed in the orientation of boundaries relative to axes a and b (see above).

Let us compare the thicknesses of fabricated YBCO films in samples type A, B, C, and D with fundamental length scales: London penetration depth $\lambda_{ab}(0)$ and superconducting coherence length $\xi_{ab}(0)$. The following values are typical for this HTSC compound: $\lambda_{ab}(0) = 139$ nm [14] and $\xi_{ab}(0) = 1.6$ nm [15]. Thus, thicknesses d of the studied superconducting films fall within the interval of

$\xi_{ab}(0) < d \ll \lambda_{ab}(0)$, which corresponds to the limit of thin (or even ultrathin) superconducting films (see, e.g., [1]).

3. Experimental research methods

Two experimental non-contact techniques were used in the present study. Brief descriptions of each of them are presented below.

A technique for local measurement of the nonlinear microwave response of a superconductor with a near-field probe with inductive coupling was used in the majority of our experiments [16]. This method allows one to study the generation of the third harmonic of the fundamental frequency by a superconductor in a wide temperature range (4–90 K). A microwave generator is the source of a signal with its frequency ranging from 0.03 to 1.2 GHz. In experiments, the first harmonic frequency was fixed at 472 MHz. This microwave signal was fed via a coaxial cable to the probe (a copper wire 50 μm in diameter and 1 mm in length). High-frequency current, which produced a quasistatic magnetic field localized on scales of the order of the probe size, was generated as a result. In the process of interaction of the high-frequency field with the examined sample, higher harmonics of the fundamental frequency formed in the reflected signal spectrum due to the nonlinear properties of the superconductor. It should be noted that the near-field probe was used both to generate the microwave field and to record the response of the superconductor to electromagnetic radiation. To prevent electric contact of the probe with the studied sample, which results in generation of a spurious signal at the frequency of the third harmonic, the sample was covered with a Teflon film 10 μm in thickness. A positioning system was also used in experiments for scanning the sample in the film plane. This system was controlled mechanically with special screws.

The second (inductive) method used here is relevant to the study of linear properties of samples (the „2 coils“ method [3,4]). The film examined in these experiments was placed between two coils (transmitting and receiving). An alternating high-frequency (30 kHz) magnetic field was generated in the transmitting coil and measured by the receiving coil. At temperatures below the critical one, the magnetic field generated by the first coil is screened strongly by the superconducting film under study. As a result, the magnetic field received by the second coil is suppressed heavily, which is manifested in the emf signal of this coil. Thus, we studied the behavior of the London penetration depth within a wide temperature range (from 100 to 2 K). The use of a special pump and a withdrawal technique made it possible to reach temperatures lower than the boiling point of liquid helium (4.2 K). It should be noted that this experimental technique is integral, since it allows one to record the linear response of a superconductor not locally, but from the entire film surface.

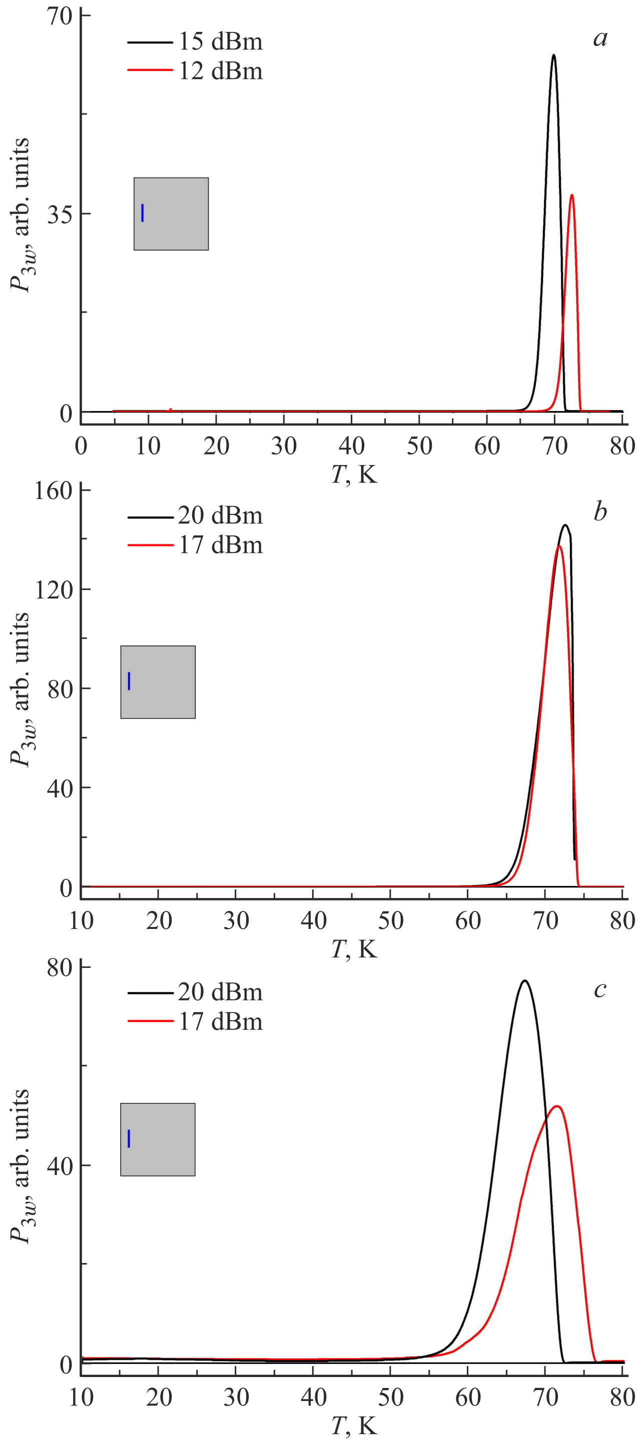

Figure 2. Dependences $P_{3w}(T)$ for samples type A with different YBCO film thicknesses: (a) $d = 20$ nm, (b) $d = 17$ nm, and (c) $d = 10$ nm. The driving powers are specified in each case. The orientation of the probe relative to the boundary is also indicated.

4. Results and discussion

Let us start this section from the presentation temperature dependences of third harmonic power P_{3w} obtained in nonlinear near-field microwave microscopy experiments.

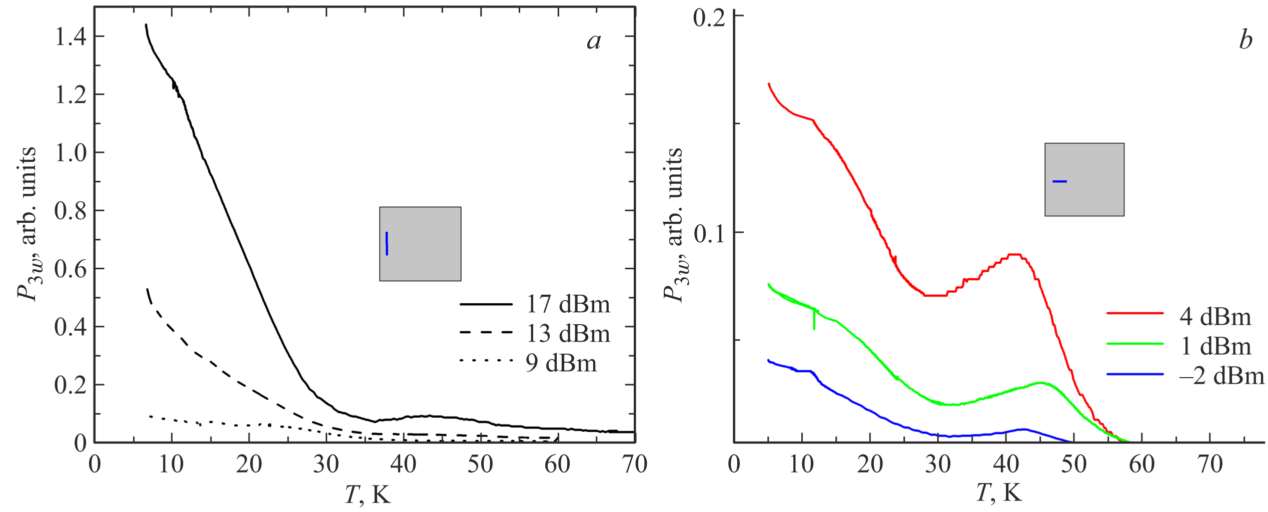

Figure 3. Dependences $P_{3w}(T)$ for samples type A with YBCO film thickness $d = 2$ nm measured with the probe oriented along the boundary (*a*) and perpendicular to it (*b*). The driving powers are specified in each case.

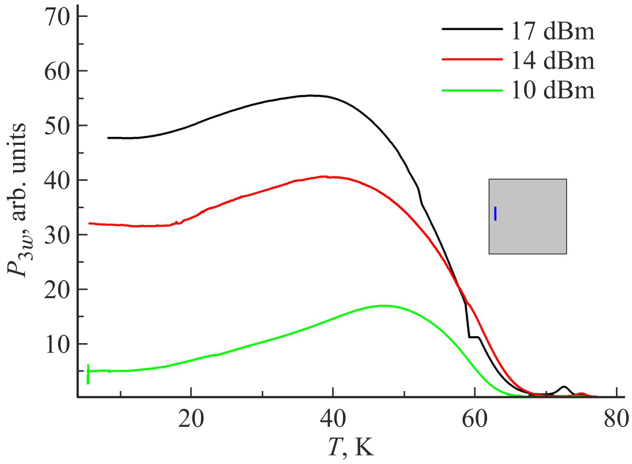

Figure 4. Dependence $P_{3w}(T)$ for sample type B with YBCO film thickness $d = 2$ nm measured with the probe oriented along the boundary. The driving powers are specified.

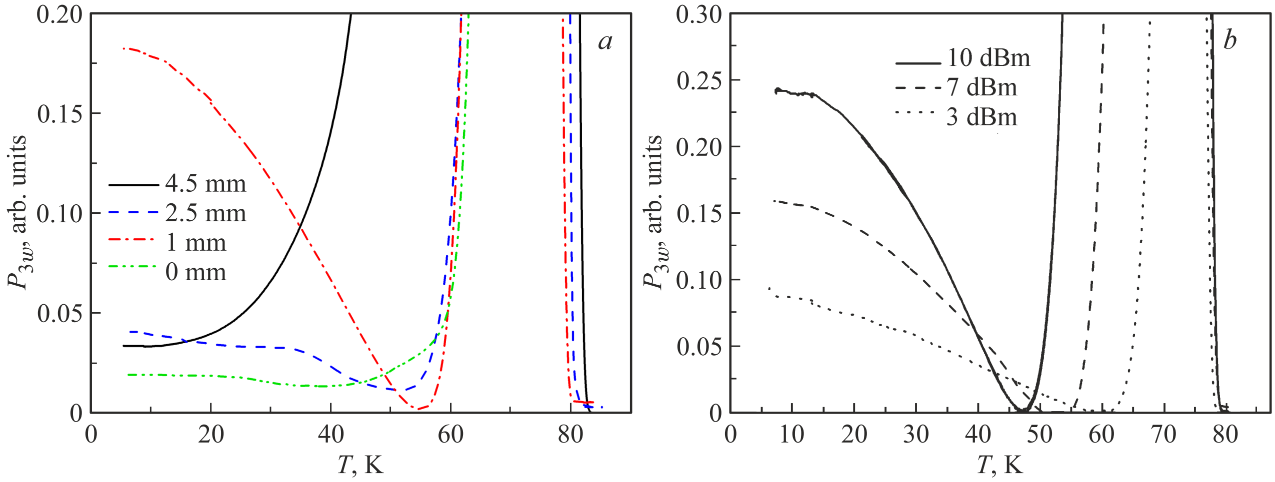

Figure 5. Dependences $P_{3w}(T)$ for samples type A with YBCO film thickness $d = 6$ nm. (*a*) Dependencies at different points along a line passing through the center of the film perpendicular to the boundary near which the nonlinear signal was studied. Distances to the location of the probe are indicated in millimeters (starting from the boundary itself, which corresponds to 0 mm); (*b*) dependences for the probe location (1 mm from the boundary) for different input powers (their values are indicated). The probe was oriented along the boundary.

Figure 2 shows the $P_{3w}(T)$ dependences for samples type A with thicknesses $d = 20$, 17, and 10 nm. Two plots corresponding to different driving powers (indicated in Figure 2) are presented for each sample. All three samples feature a single sharp peak near critical temperature T_c. The critical temperature is understood here as the maximum temperature below which nonlinearity arises (see [16] for details). As was noted in Introduction, technical limitations of the available measuring equipment make it impossible to isolate the signal from noise when the temperature drops to 4 K. As the film thickness decreases, the peak gets shorter and broader. This is seen most clearly when one compares the plots corresponding to $d = 17$ nm (Figure 2, *b*) and $d = 10$ nm (Figure 2, *c*) and the same input power values (17 and 20 dBm). Notably, critical temperature T_c remains virtually unchanged in all three films. It assumes a value around 75 K in each film and varies slightly (within 5 K) with the amplitude of the input signal. It should be noted that the same probe orientation (the excitation current flowed parallel to the boundary near which the nonlinear response was recorded; this is indicated in Figure 2 in each panel) was used in these examples.

A qualitatively different pattern is found in thinner YBCO films. Figure 3 shows the $P_{3w}(T)$ plots for samples type A with YBCO film thickness $d = 2$ nm. These plots differ in orientation of the probe relative to the boundary (indicated in the figure in each case). A nonlinear signal, which increases with decreasing T, is seen at low temperatures against the background of a fairly broad peak of a moderate height. This pattern is preserved at various input power levels (indicated in the figure). Note that the nonlinear signal in Figure 3, *a* (with the probe oriented along the boundary) is substantially more intense than in Figure 3, *b*. The discovered feature is indicative of local amplification of supercurrent near the boundary, which is substantiated by the results of analytical calculations performed in [16].

This effect may be caused by the formation of Andreev bound states near the film boundaries (specifically, near the one where the measuring probe is located; see the introduction and text in [13]), since the YBCO film boundaries in this sample are oriented at an angle of 45° to axes *a* and *b*. To verify this assumption, we performed similar studies for samples type B with thickness *d* of the YBCO film also being equal to 2 nm and axes *a* and *b* of the YBCO film directed along/perpendicular to the sample boundaries (see the plots in Figure 4). It can be seen that the nonlinear signal in this case does not grow more intense as the temperature decreases.

Similar studies were carried out for samples type A with slightly thicker YBCO films ($d = 6$ nm). Figure 5, *a* shows the $P_{3w}(T)$ dependences for a given input power obtained at different points along a line passing through the center of the film perpendicular to the boundary near which the nonlinear signal was studied. The probe was also oriented parallel to the boundary. The distances to the probe location (starting from the boundary itself, which corresponds to

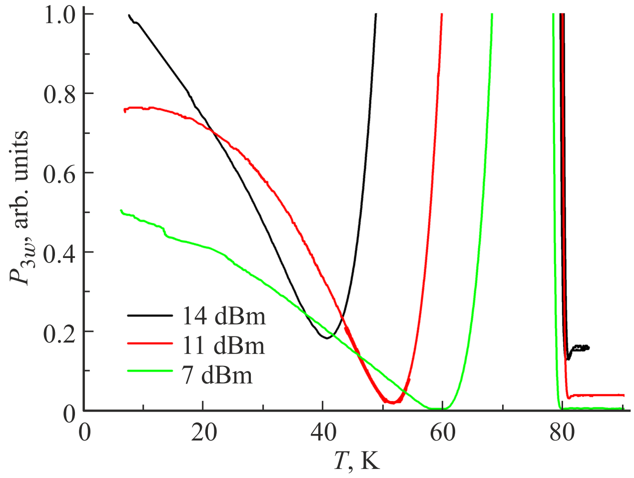

Figure 6. Dependences $P_{3w}(T)$ for sample type C with YBCO film thickness $d = 4$ nm measured with the probe oriented along the boundary. The driving powers are specified.

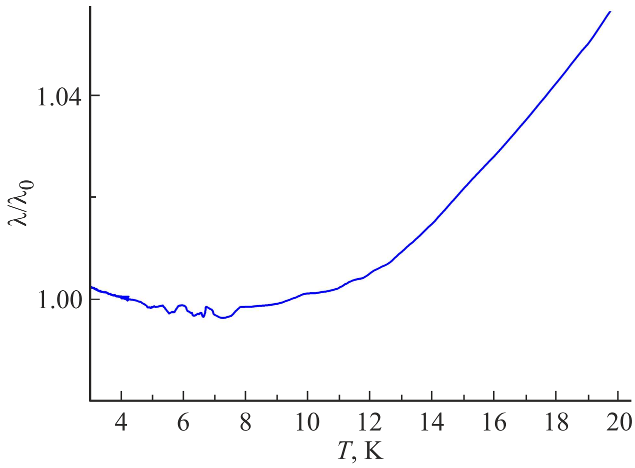

Figure 7. Temperature dependence of normalized London penetration depth $\lambda(T)/\lambda_0$, where $\lambda_0 = \lambda(T = 4\,\mathrm{K})$.

0 mm) are indicated in Figure 5, *a*. Owing to the above-mentioned electrodynamic signal amplification, the most profound effect is observed at a distance of approximately 1 mm from the boundary. Additional studies of the nonlinear response corresponding to different input powers were also carried out at this probe position (see Figure 5, *b*). In all these examples, $P_{3w}(T)$ increases significantly with a reduction in temperature.

Samples type C and D were then studied by nonlinear near-field microwave microscopy. It was already noted that the YBCO film in these samples had thickness $d = 4$ nm. As expected, the third harmonic power did not increase at lower temperatures for samples type D (with axes *a* and *b* directed along/perpendicular to the boundaries). In samples type C (with axes *a* and *b* oriented at an angle of 45° to the boundaries), $P_{3w}(T)$ increased with decreasing temperature, which is demonstrated in Figure 6. The probe in this case was oriented along the boundary and positioned at a distance of approximately 2 mm from it. The effect is expected to be even more profound in a thinner YBCO film: the high-temperature phase should be suppressed, and only the peak corresponding to $T_c \approx 60$ K (low-temperature phase) would remain in the $P_{3w}(T)$ dependence.

Inductive measurements by the „2 coils“ method were also carried out for samples type C. Figure 7 presents the dependence of the London penetration depth (in relative units) on temperature. It can be seen that the London penetration depth increases at temperatures below 7−8 K. The discovered feature of the $\lambda(T)$ dependence may also be attributed to the presence of Andreev states (see similar results in [9,10]).

The probable observation of Andreev states in sample type C is rather unexpected, since, owing to natural limitations of sputtering technology, the YBCO film boundaries in it are of a significantly lower quality than those in samples type A and B (see the above discussion of fabrication specifics). Though, the effect is still observed.

5. Conclusion

The nonlinear response and the London penetration depth of YBCO thin films were found to increase with decreasing temperature. The observed effect may be attributed to the presence of Andreev states emerging near the optimally oriented film boundaries. Further investigation of this effect with the use of nonlinear near-field microwave microscopy offers opportunities in the field of, e. g., experimental determination of the type of superconducting pairing in thin films of different superconductors.

Acknowledgments

The authors thank A.S. Mel’nikov for numerous discussions of the results of this study and useful advice and suggestions.

Funding

This study was carried under the state assignment of the Institute of Applied Physics of the Russian Academy of Sciences. Equipment provided by the common use center of the Institute of Physics of Microstructures of the Russian Academy of Sciences was used in experiments.

Conflict of interest

The authors declare that they have no conflict of interest.

References

[1] D. Saint-James, G. Sarma, E.J. Thomas. Type II Superconductivity. Pergamon. N. Y. (1969).
[2] P.J. Hirschfeld, N. Goldenfeld. Phys. Rev. B **48**, 4219 (1993).
[3] J.H. Claassen, M.E. Reeves, R.J. Soulen. Rev. Sci Instrum. **62**, 996 (1991).
[4] A.V. Antonov, A.I. El’kina, B.K. Vasiliev, M.A. Galin, D.V. Masterov, A.N. Mikhaylov, S.V. Morozov, S.A. Pavlov, A.E. Parafin, D.I. Tetelbaum, S.S. Ustavschikov, P.A. Yunin, D.A. Savinov. Phys. Solid State **62**, *9*, 1598 (2020).
[5] C.R. Hu. Phys. Rev. Lett. **72**, 1526 (1994).
[6] R.J. Cava, A.W. Hewat, E.A. Hewat. Physica C **165**, 419 (1990).
[7] M. Aprili, E. Badica, L.H. Greene. Phys. Rev. Lett. **83**, 4630 (1999).
[8] R. Prozorov, R.W. Giannetta. Supercond. Sci. Technol. **19**, R41 (2006).
[9] A. Carrington, F. Manzano, R. Prozorov, R.W. Giannetta, N. Kameda, T. Tamegai. Phys. Rev. Lett. **86**, 1074 (2001).
[10] H. Walter, W. Prusseit, R. Semerad, H. Kinder, W. Assmann, H. Huber, H. Burkhardt, D. Rainer, J.A. Sauls. Phys. Rev. Lett. **80**, 3598 (1998).
[11] S.K. Yip, J.A. Sauls. Phys. Rev. Lett. **69**, 2264 (1992).
[12] T. Dahm, D.J. Scalapino. Appl. Phys. Lett. **69**, 4248 (1996).
[13] A. Zare, T. Dahm, N. Schopohl. Phys. Rev. Lett. **104**, 237001 (2010).
[14] A. Schiling, F. Hulliger, H.R. Ott. Physica C **168**, 272 (1990).
[15] U. Welp, W.K. Kwok, G.W. Grabtree, K.G. Vandervoort, J.Z. Liu. Phys. Rev. Lett. **62**, 1908 (1989).
[16] A.Yu. Aladyshkin, A.A. Andronov, E.E. Pestov, Yu.N. Nozdrin, V.V. Kurin, A.M. Cucolo, R. Monaco, M. Boffa. Radiophys. Quantum Electron. **46**, *2*, 109 (2003).

Translated by D.Safin